京都大学防災研究所年報 第40号 B-1 平成9年4月
Annuals of Disas. Prev. Res. Inst., Kyoto Univ., No. 40 B-1, 1997

Magma Transport at Mt. Unzen Associated with the 1990－1995 Activity Inferred from Leveling Data

Muhamad HENDRASTO*, Tsuneo ETO, Fumiaki KIMATA**,
Takeshi MATSUSHIMA*** and Kazuhiro ISHIHARA

*Graduate School of Science, Kyoto University
**Faculty of Science, Nagoya University
***Faculty of Science, Kyushu University

Synopsis

The recent activity of Mt. Unzen (Fugendake) was preceded by an earthquake swarm beneath the Tachibana Bay, west of the Shimabara Peninsula, in November 1989 and the subsequent migration of seismic activity toward Mt. Unzen. On November 17, 1990, phreatic eruption started at the summit, then a dacite lava dome appeared at the summit crater on May 20, 1991. Subsequent discharge of lava and intermittent pyroclastic flows have continued until early 1995. The total volume of discharged lava was 0.2 km^3. Universities and the Geographical Survey Institute had repeated leveling survey along the western coast of the peninsula, and the other route from the northern flank to the summit, and found out significant deflation of the ground centered a few kilometer west of the summit, which was also clarified by GPS survey. The magma supply system composed of three chambers, and an inclined magma pathway along seismic zone were proposed by previous studies.

Applying the Point-Source Model (Mogi's Model), the location of three pressure sources and their intensity change with time were re-examined including the evaluation of measurement error of leveling data, and the relationship between the intensity changes at pressure sources and volcanic activity.

(1) The near surface source A is located at a depth of 1.4 km beneath the summit, and the source B is 4.1 km deep, 3 km west of the summit. And the deepest one C is located 6.8 km deep, west of the summit. These sources are aligned just beneath the inclined seismic zone.

(2) The intensity change at A-source seems to be related to the discharge rate of lava and seismic activity at the summit.

(3) The intensity change at B-source has two peaks corresponding to the two epochs of discharge of lava and increased prior to the onset of discharge of lava. The intensity of C source increased until the lava dome appeared, and then gradually decreased.

(4) These results suggest magma was transported from C-source through B- and A-sources to the summit. Assuming the deformation volume of the ground surface due to pressure sources is equal to the volume change of magma at each source, the supply rate of magma from deeper portion to C-source was estimated using the data on discharge lava. The supply rate of magma increased rapidly after the phreatic eruption in November 1990, and reached its peak in the end of 1991, then decayed. In early 1995, magma supply stopped. The total volume of magma supplied since 1990 is estimated to be 0.17 km^3

Keywords: Mt. Unzen; leveling; pressure source; magma supply; lava dome

1. Introduction

Mt. Unzen, an active volcano located on the Shimabara Peninsula southwest Japan, is a volcano consisting mainly of dacitic rock. The volcano is situated in a depression zone trending to E-W direction, called as Unzen Graven, among the Chijiwa Fault (north) and the Kanahama and Futsu Faults (south) (Ohta, 1993). The recent activity started with a sequence of earthquake swarm beneath the Chijiwa Bay to the west of Mt. Unzen in November 1989. Then the hypocenters migrated eastward with time and became shallower toward Mt. Unzen (Ohta *et al.*, 1992; Shimizu *et al.*, 1992). at Jigokuato and Kujukushima craters on November 17, 1990, after a repose period of 198 years. Even after the eruption, earthquakes sometimes occurred beneath the western flank, and intermittent eruptions occurred until the beginning of May. Very shallow volcanic earthquakes and tremors began to occur beneath the summit craters on May 13, 1991. Then dacite dome appeared in Jigokuato crater on May 20, 1991. This lava dome continued to grow up until the early 1995. The cumulative volume was estimated to be 0.2 km^3 as of February 1995 (Geographical Survey Institute, 1994).

Shallow magma supply system has been discussed from geochemical, seismological and ground deformation studies. Ohta (1993) proposed pathway of magma from the Chijiwa Bay across the Shimabara Peninsula based on geochemical study of hot springs and hypocentral distribution of earthquakes.

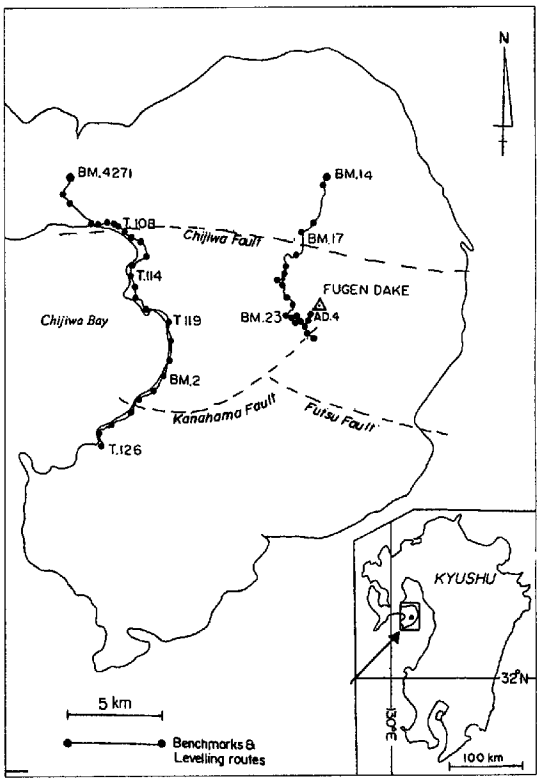

Fig. 1 Location map of leveling routes in the Unzen area, Shimabara Peninsula

Joint Research Team of Mt. Unzen and Geographical Survey Institute have repeated leveling and GPS surveys at Mt. Unzen since 1991. Leveling surveys have been carried out along two independent routes. The one runs along the western coast of the Shimabara Peninsula, and the other does from the northern flank toward the summit of the Mt. Fugen

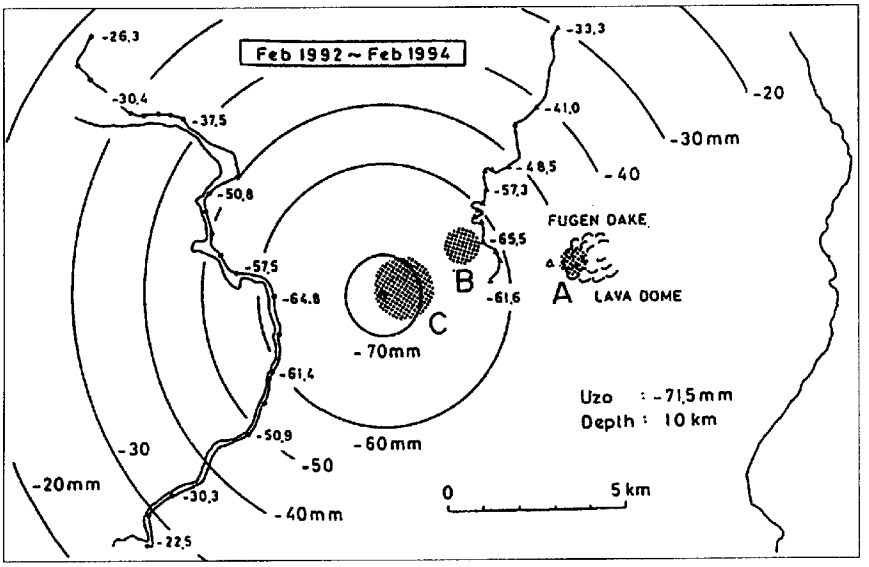

Fig. 2 Vertical displacement in the deflation storage by magma discharge at Mt. Unzen (Geodetic Survey Party, 1994).

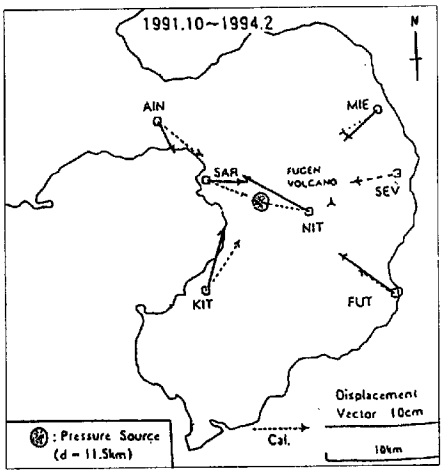

Fig. 3 Horizontal displacement in the deflation stage by magma discharge at Mt. Unzen (Nishi *et al.*, 1995).

(Fig. 1). From the analysis of leveling data, Ishihara (1993) proposed the magma chambers system denoted by A, B and C sources (Fig. 2). The pressure source found from GPS surveys was coincided with the C source, in the horizontal location (Fig. 3), but located at a few kilometers deeper (Nishi *et al.*, 1995).

The problem of the previous model (Ishihara, 1993) is independent determination of B and C sources, that is to say, the B source (about 5 kilometers deep) was obtained only from the data of the northern flank route during the early stage of eruption in 1991, and later the C source (about 7 kilometers deep) was determined from the analysis of the data along the western coast.

In this study, we try to relocate the pressure sources, using the leveling data both of the western coast and the northern flank lines of Mt. Unzen, and

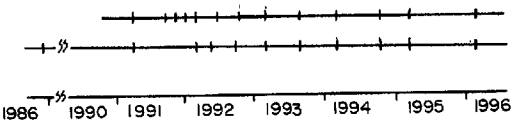

Fig. 4 Measurement times of leveling surveys at north slope of Mt. Unzen (upper part), and west coast of Simabara Peninsula (lower part), respectively.

Table 1 Results for calculated parameters.

Location of Pressure sources			
	A	B	C
X (km)	2.7	0.3	-2.4
Y (km)	3.6	4.4	2.6
f (km)	1.4	4.1	6.8

Date	Intensities (10 m)			Reference points (mm)		
	A	B	C	BM. 4271	BM. 14	BM. 23
November 1986	-	-	-2.3075	-0.1	-	-
November 1990	-	-	-1.7142	-0.2	-	-
March 1991	-	0	0	0	0	-
May 1991	0	-	-	-	-	0
June 1991	-0.0249	-	-	-	-	-2.8
July 1991	-0.0439	-	-	-	-	-4.9
August 1991	-0.10187	0.4375	-1.5717	-	-3.4	-11.7
October 1991	-0.05749	0.3132	-2.4855	-	-8.6	-6.5
December 1991	-0.02648	0.4064	-3.1007	-	-11.0	-3.3
February 1992	-0.03159	0.3224	-3.1272	-1.4	-11.6	-3.8
May 1992	-0.0671	0.0367	-3.9351	-3.7	-18.5	-7.8
September 1992	-0.0696	0.0192	-3.731	-7.2	-17.6	-8.0
February 1993	-0.0388	0.0705	-3.8765	-6.5	-17.9	-4.6
August 1993	-0.0914	0.1538	-5.2992	-9.0	-24.0	-10.4
February 1994	-0.0579	0.4155	-6.2203	-12.5	-25.2	-6.9
September 1994	-0.06915	-0.033	-5.7646	-13.6	-28.0	-8.2
January 1995	-0.0728	-0.0028	-5.5698	-12.0	-26.8	-8.5
February 1996	-0.0794	0.0267	-5.9746	-12.5	-28.4	-9.3

	Two point sources model	Single point source model
WSSR (mm)	303.9	735.6
Correlation Coefficient	0.9843	0.8847

Intensities, location of B and C Sources and reference points at BM. 4271 and BM. 14, derived from two point sources model. Intensity, location of A source and reference point at BM. 23, derived from single point-Source Model (Origin point: 130° 16' E, 32° 43.58' N).

propose the refined magma chambers model to discuss the magma supply system associated with the eruptive activities of the volcano.

2. Measurement

2.1 Data

Geodetic monitoring of Unzen Volcano using precise leveling was started in November1986 at the west side of the volcano (along western coast of Shimabara Peninsula) by University Team. The second measurement was done in November 1990 by the Geographical Survey Institute. Additional leveling route was made at the northern flank of Mt. Unzen from north side (BM.14) to Azamidani (BM. AD.4). After the eruption in 1990 leveling survey has been repeated twice per year for both two routes (Fig. 4).

The section height difference (relative elevation difference between adjacent benchmarks) dh_i is defined by the height of the forward benchmark (h_i) and the previous benchmark (h_{i-1}), as follows:

$$dh_i = h_i - h_{i-1} \quad (1)$$

The elevation at ith benchmark (h_i) is calculated by summing all the section height differences (dh_i) from the reference benchmark (BM.4271 and BM 14 for western coast and northern flank leveling routes, respectively) to the ith benchmark (Table 1).

$$Hi = \Sigma dh_i \quad (2)$$

Height change of the ith benchmark (Δhi) is calculated by subtracting the former benchmark elevation $h_i(t_1)$ from the later elevation, $h_i(t_2)$.

$$\Delta h_i = h_i(t_1) - h_i(t_2) \quad (3)$$

2.2 Leveling error

Leveling measurement may be contaminated by measurement errors. During leveling surveys, the successive sections are generally measured twice. The forward and backward height difference between the benchmarks are usually slightly discrepant. Bomford (1971) states that the random error should propagate as :

$$\delta_i = \alpha L_i^{1/2} \quad (4)$$

where, L_i is distance along the leveling route in km, and α is mean square error, in mm/km which is computed from several double-run sections.

Universities and Geographical Survey Institute computed mean square errors α of west coast and north slope leveling surveys to be 0.4 - 0.7 mm/km. These were then used to obtain the cumulative random error on a leveling lines. The cumulative

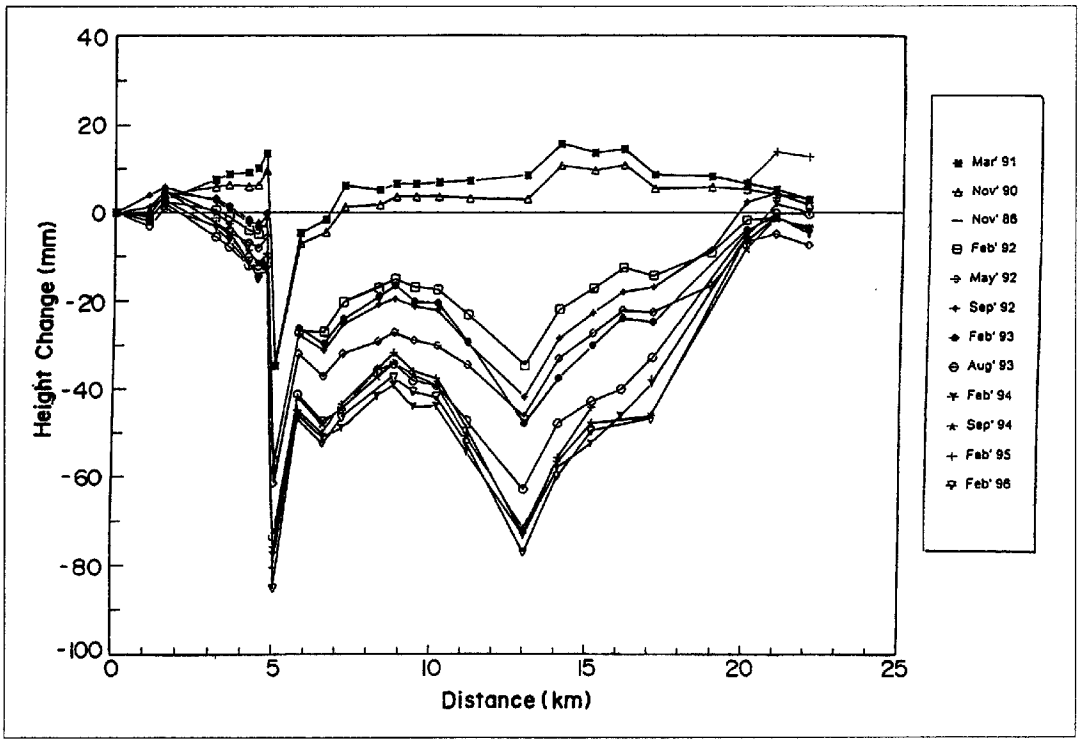

Fig. 5 Vertical displacements of benchmarks along the western coast of Shimabara Peninsula, referred to BM. 4271 and to March 1991.

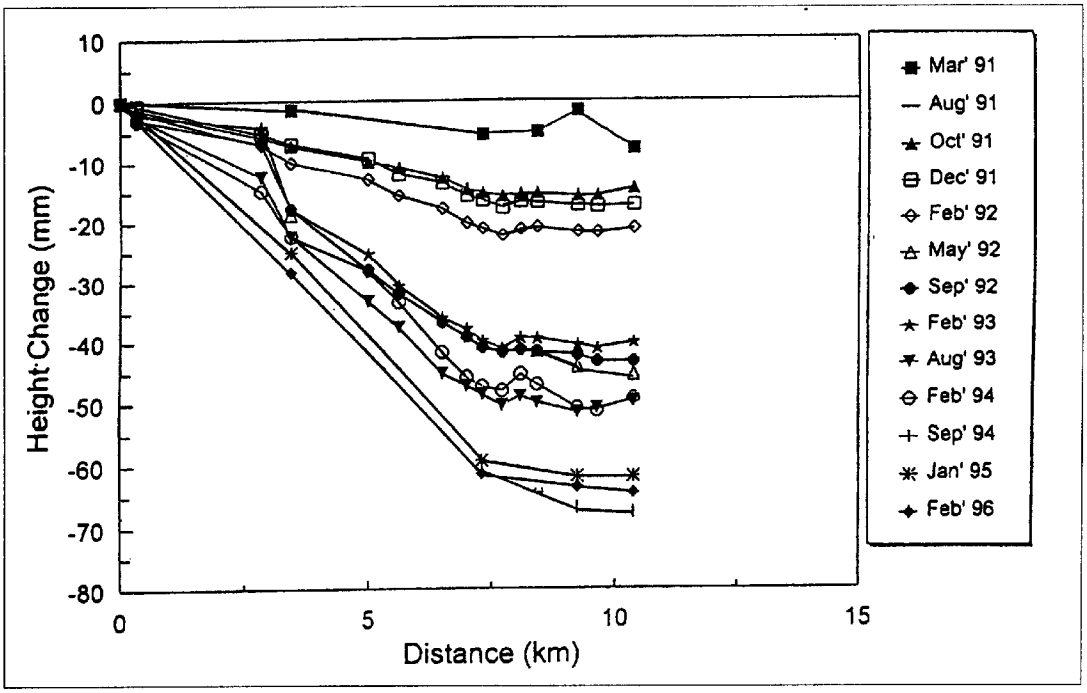

Fig. 6 Vertical displacements of benchmarks along the northern frank of Mt. Unzen, referred to BM. 14 and to March 1991.

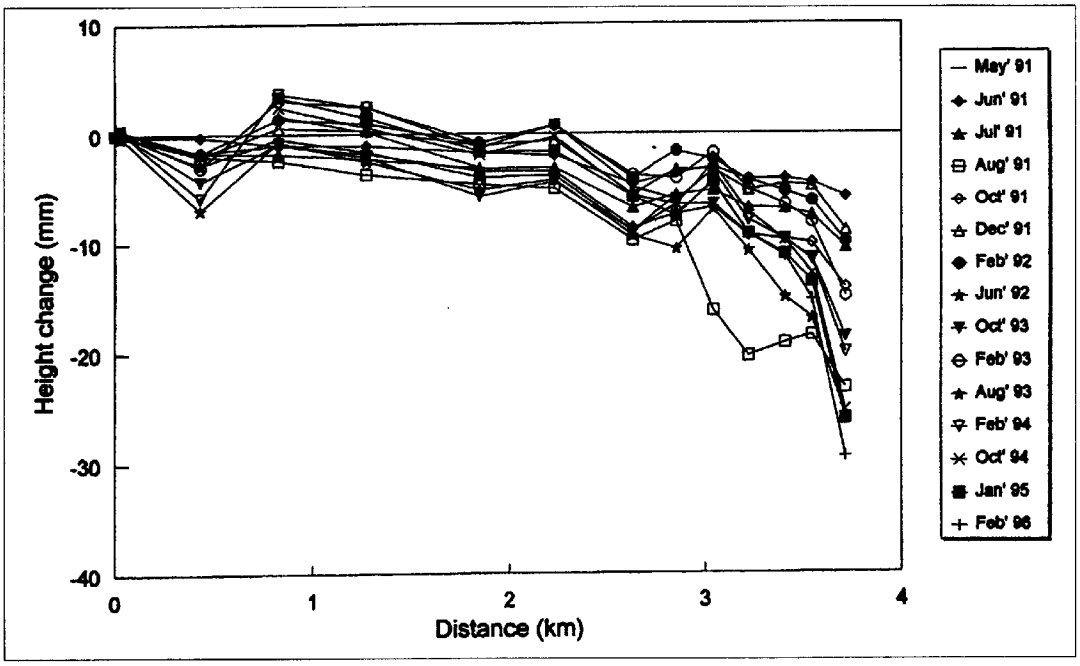

Fig. 7 Vertical displacements of benchmarks along the western frank of Mt. Unzen, referred to BM. 23 and to March 1991.

random error for height changes measured between two the surveys t_1 and t_2 is given by:

$$\delta_t = (\alpha_1 + \alpha_2)^{1/2} L_i^{1/2} \quad (5)$$

where α_1 and α_2 denote the mean square errors of the first and second measured elevation of t_1 and t_2, respectively.

3. Analysis

Before the lava dome appearance on May 20, 1991, the volcano was inflating, then turned to deflating. This phenomena is clearly recognized by the height changes of benchmarks at the western coast, the northern flank and the near-summit

leveling lines, respectively (Figs. 5, 6 and 7). It is noteworthy that each leveling line shows the different pattern of height changes as shown in Fig. 8. Therefore, it is difficult for us to explain the ground deformation at Mt. Unzen by using Single-Source Model.

We estimate locations and source intensities of the two pressure sources, assuming Point-Source Model (Mogi, 1958), from western coast (BM.4271 to BM. T.126) and northern flank (BM.14 to BM.23) data (Fig. 9). The procedure of our analysis is described as follows:

If hydrostatic pressure change occurs in sphere under the earth's surface in an ideal semi-infinite elastic body, the surface is deformed symmetrically around the embedded sphere center. Vertical displacements (Δh_i) at the point (x, y) due to two pressure sources may be represented as follows:

$$\Delta h_i = K_B \frac{f_B}{\left(r_B^2 + f_B^2\right)^{2/3}} + K_C \frac{f_C}{\left(r_C^2 + f_C^2\right)^{2/3}} \quad (6)$$

where r_B and, r_C: are horizontal distances from the

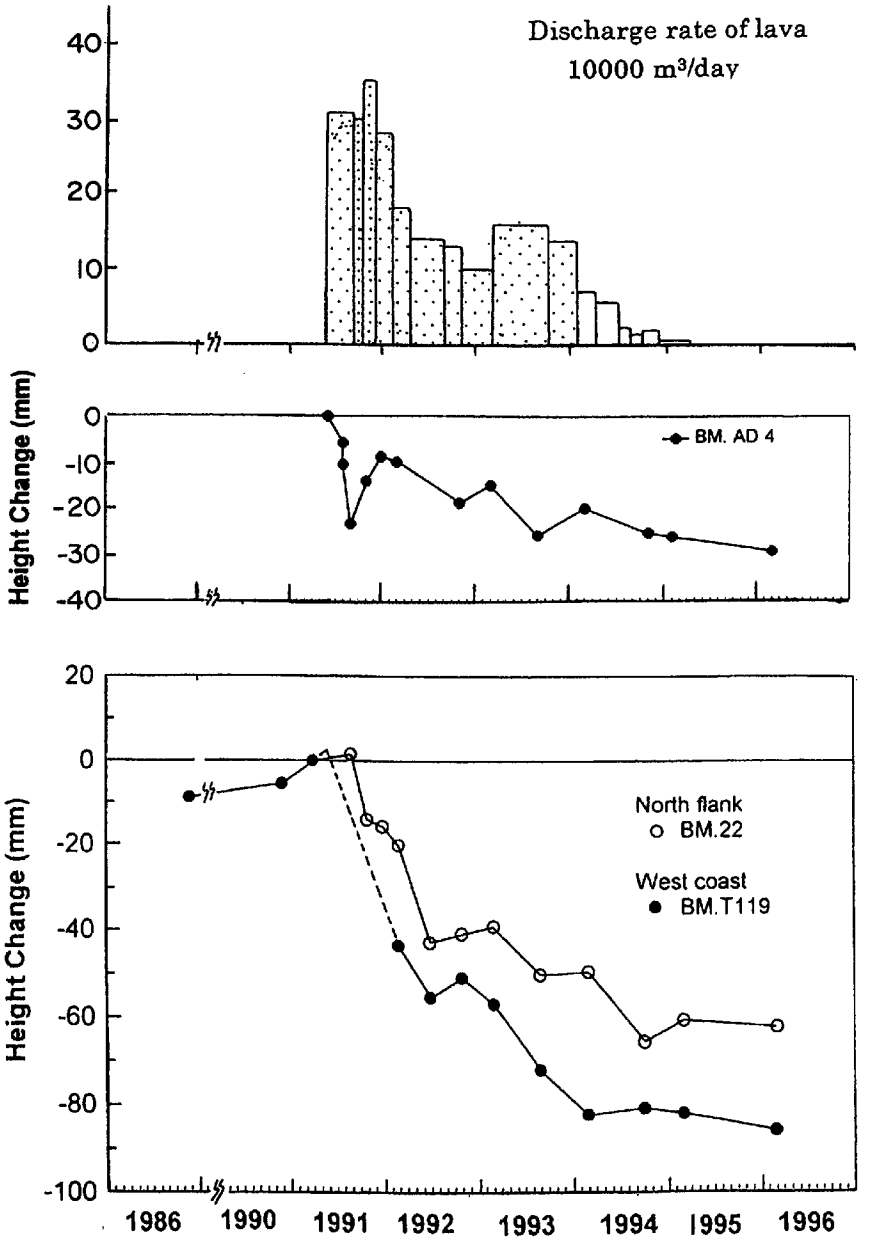

Fig. 8 Upper: Discharge rate of lava. Middle: vertical displacement of benchmark AD. 4 (referred to BM. 23), the nearest benchmark T. 119 (referred to BM. 4271 and to March 1991), at the western coast of Shimabara Peninsula, and those of benchmark 22 (referred to BM. 14 and to March 1991) at northern flank of Mt. Unzen.

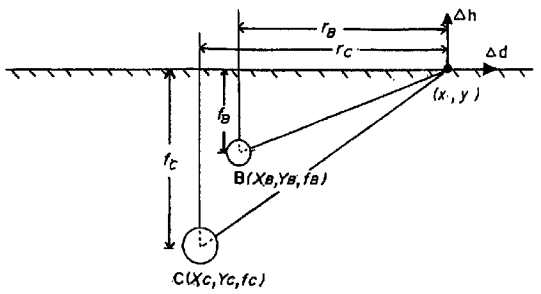

Fig. 9 Point Source Model with two pressure sources for the deformation analysis of geodetic data. The hydrostatic pressure change on the two embedded spheres reside at depths f_B and f_C. Pressure perturbations at depths induced radial (Δd), and vertical (Δh) displacement components at varying radii (r) from the two epicenters of inflation.

center of inflation/deflation (B and C) to measurement points,

$r_B = \{(x-x_B)^2+(y-y_B)^2\}^{1/2}$,

$r_C = \{(x-x_C)^2+(y-y_C)^2\}^{1/2}$,

x, y: coordinate of benchmarks,

f_B, and f_C: are depth from the surface to the center of the sources B and C, and, K_B, K_C: intensities at the sources B and C, represented as,

$$K_B = \frac{3a_B{}^3\Delta P_B}{4\mu}, \quad K_C = \frac{3a_C{}^3\Delta P_C}{4\mu},$$

where $\mu(=\lambda)$ is Lame's constants, a_B, a_C are radius of pressure sources, ΔP_B and ΔP_C are changes of the hydrostatic pressure in the sources B and C.

To find out the best-fit location of the pressure sources, we calculate the weighted sum of squares residual (WSSR) incorporating the estimate of error (δ_i, from eq. (4)), between the observation and the model calculation for the both west coast and north flank data at six measurement periods of the interval between February 1992 to February 1996. Calculation was done according to the following procedure:

[1] The locations of the two pressure sources are estimated by using grid searching method. The grid (size: 0.1 km) are arranged in the area of 7x7 km around Mt. Unzen and 1 to 9 km depth.

[2] Under given locations of the two pressure sources, the parameters K_B, K_C, ho_w and ho_{nf} for 6 periods are estimated by least squares to minimize the misfit between the observations and the calculated height changes, using the eq. (7).

[3] The best-fit locations and parameters are determined at the minimum of *WSSR* over the grid searching scheme.

$$WSSR = \left[\sum_i^n\left(\frac{\Delta h_{i,w(obs)} + ho_w - \Delta h_{i,w(cal)}}{\sigma_{i,w}}\right)^2 + \sum_i^n\left(\frac{\Delta h_{i,nf(obs)} + ho_{nf} - \Delta h_{i,nf(cal)}}{\sigma_{i,nf}}\right)^2\right]_{Period1} + \cdots + \left[\sum_i^n\left(\frac{\Delta h_{i,w(obs)} + ho_w - \Delta h_{i,w(cal)}}{\sigma_{i,w}}\right)^2 + \sum_i^n\left(\frac{\Delta h_{i,nf(obs)} + ho_{nf} - \Delta h_{i,nf(cal)}}{\sigma_{i,nf}}\right)^2\right]_{Period6} \quad (7)$$

where, *obs*, *cal* refer to observed and calculated height changes, respectively, the subscript w and n_f refer to west coast and north flank, respectively, n is number of data, σ is the cumulated error and *ho* is the height changes at the fix point (as mentioned before, the observed data give us only the relative height change, in such a case, we added one parameter, *ho*, to each leveling line data).

In addition, we also examine Single-Source Model (denoted by A) to local ground deformation around Fugendake using the leveling data of the Fugendake. To find out the best-fit location of the source A, we calculate the *WSSR* incorporating the estimate of error (σ_i, from eq. (4)) between the observation and the model calculation for Mt. Fugen data (BM. 23 to BM. AD.4) at thirteen measurement periods of the interval between May 1991 to February 1996. Calculation was done according to the following procedure:

[1] The locations of the pressure source are estimated by using grid searching method. The grid (size: 0.1 km) are arranged in the area 4x4 km around the summit of Fugendake and 0-4 km in depth.

[2] Under given location of the pressure source, the parameters K_A and *ho* for 13 period are estimated by least squares to minimize the misfit between the observations and the calculated height changes.

[3] The best-fit location and parameters are determined at the minimum of WSSR over the grid searching scheme.

$$WSSR = \sum_i^n\left(\frac{\Delta h_{i,(obs)} + ho - \Delta h_{i,(cal)}}{\sigma_i}\right)^2_{Period1} + \sum_i^n\left(\frac{\Delta h_{i,(obs)} + ho - \Delta h_{i,(cal)}}{\sigma_i}\right)^2_{Period6} \quad (8)$$

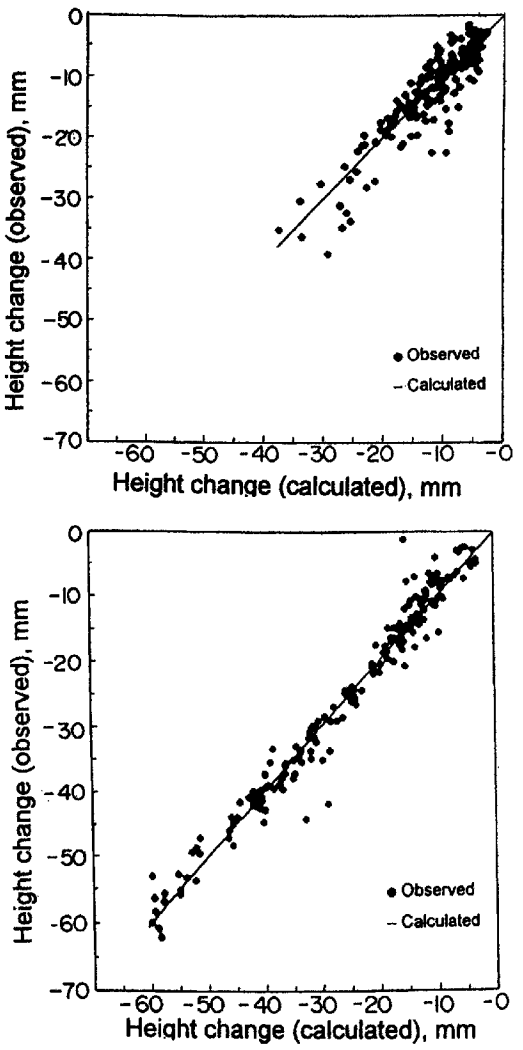

Fig. 10 Relation between the calculated height changes and the observed ones. (Top) For the Benchmarks at Mt. Fugen derived from single source model for all the measurement periods between May 1991 and February 1996. (Bottom) For the benchmarks at the west coast and north-flank derived from the two sources model for all the measurement periods between February 1992 and February 1996.

4. Results and evaluation of analysis

The results of calculated parameters are given in Table 1. The minimum of weighted sum of squares residual (WSSR) for the two pressure sources model is obtained when the location of the pressure source B is at about 3 km west of Mt. Fugendake at a depth of 4.1 km, and the pressure source C is located at about 5 km west of Mt. Fugendake at a depth of 6.8 km. The coefficient of correlation between the observed and calculated height changes is 0.9843 (Fig. 10). The minimum of WSSR for the single pressure source model using near summit leveling data is obtained when the location of the source A is at about 0.25 km north-east of Mt. Fugen at a depth of 1.4 km beneath the summit (0.6 km below sea level). The coefficient of correlation between the observed and calculated height changes, is 0.8857 (Fig. 10).

Those best-fit model have a little different with the previous studies (Ishihara, 1993), the location of the pressure source C (deeper one) obtained from this study coincides with the previous studies, and the pressure source B and A was located about 1 and 0.5 km shallower than that of the previous study, respectively, as shown in Fig. 11.

5. Discussion

Physical meaning of the location of three pressure sources (A, B and C) in relation to the eruptive activities of Mt. Unzen is discussed below. First we show the relationship between hypocenters of earthquakes and the location of pressure sources.

If we compare the location of the three pressure sources with the hypocenter distribution of

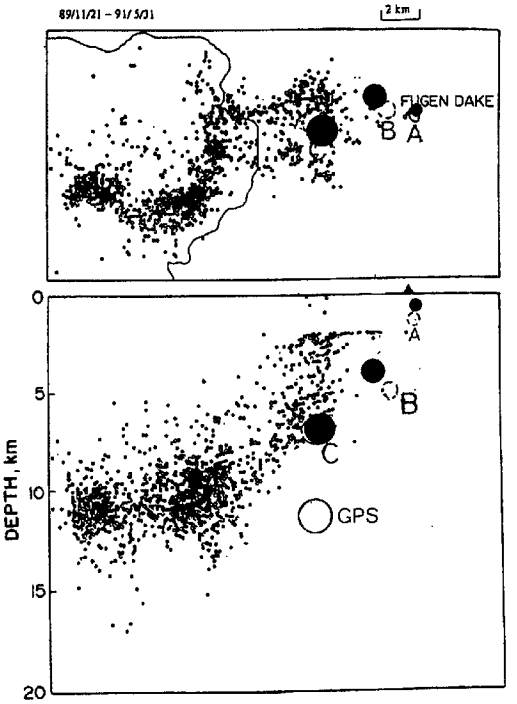

Fig. 11 Schematic map of Unzen area, Shimabara Peninsula, showing locations seismic zones (Umakoshi *et al.*, 1995). Solid circles show the best- fit models in our study. Dashed circles show the best-fit model from Ishihara (1993) and open circle from GPS data (Nishi *et*

earthquakes (Umakoshi *et al.*, 1995), we may point out that the estimated pressure sources A, B and C are located beneath the inclined seismic zone (Fig. 11). This relationship may be reasonable. If pressure sources A, B and C corresponded to magma chambers filled with magma, stress will not be accumulated and earthquakes will not occur at pressure source. And earthquakes will be generated above magma supply system to release stress due to accumulation of magma or intrusion of lava. In fact the seismicity west of Mt. Unzen had been high until early 1990, while the inflation of the ground was observed, but decayed rapidly after both the discharge of lava and deflation of the ground started.

To clarify the relationship between the pressure sources A, B, C, and the volcanic activity of Mt. Unzen, we also calculate the intensity at the sources B and C for the periods between November 1986 and February 1992 by using the best-fit locations of the two sources, then the changes of intensities at each pressure source are discussed in relation to the discharge of lava and the seismic activity.

5.1 The relationship between the near-surface pressure source and the eruptive activity

The pressure source A is located 1.4 km beneath the summit. The earthquakes at the summit were originated shallower than 1 km. Therefore it is expected that the intensity change is closely related to the discharge rate of lava or seismic activity. Fig. 12 shows the monthly number of summit earthquakes, the discharge rate of lava and the relative intensity of A-source.

The intensity of A-source gradually decayed with time, as similar as the discharge of lava did. However, we recognize short-time variations of the intensity of A-source. The variations seem to be related to those of discharge of lava or seismic activity. The increase in the relative intensity of A-source related to high seismicity or increase in discharge rate of lava. Such a variation suggests that the increase in intensity of A-source causes higher discharge of lava or higher seismicity, and repeated increase in intensity of A-source may indicate magma supply from deeper part, probably through B-source.

5.2 The relationship of deeper sources, B and C, with volcanic activity

The relative intensity changes of B and C-sources are illustrated with the discharge rate of lava

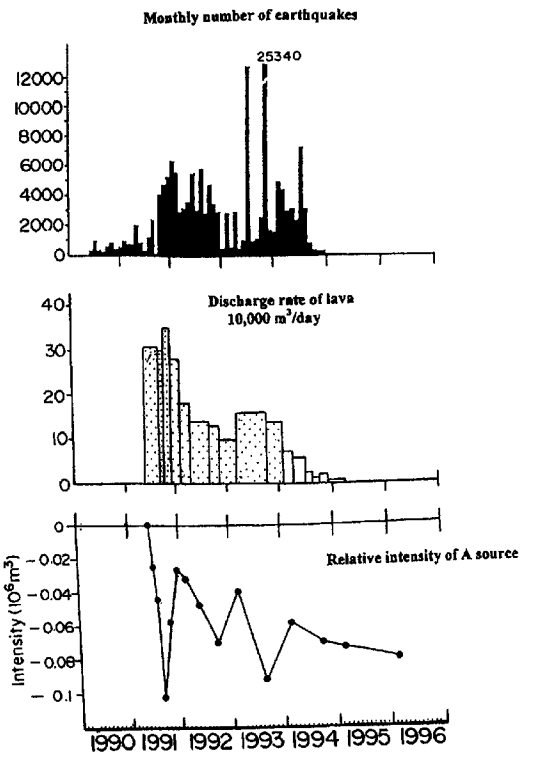

Fig. 12 Relationship between the monthly number of earthquakes (Umakoshi, 1995), discharge rate of lava (Geographical Survey Institute, 1994; Geological Survey of Japan, *et al.*, 1995) and the relative intensity of A-source, respectively.

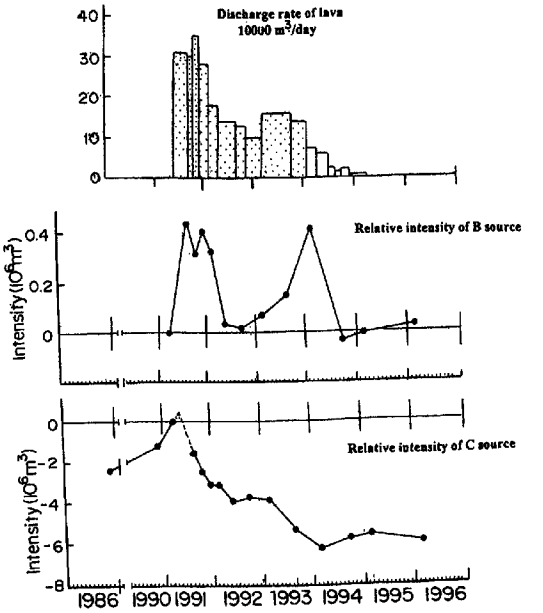

Fig. 13 Relationship between the discharge rate of lava and the relative intensities of B and C-sources, respectively.

in Fig. 13.

The relative intensity of B-source has two peaks, as corresponding to the two epochs of discharge of lava, 1991-1992 and 1993-1994, respectively. In addition it is noteworthy that the intensity increased a few months before the discharge of lava started in 1991 and again a few months before the resumed activity in March 1993. These relationship suggests that increase in the intensity of B-source is caused due to magma supply from deeper part, probably from C-source, and induced magma transport to the near-surface A-source.

The intensity of C-source had gradually increased prior to the phreatic eruption in November 1990, and increased rapidly, probably, until discharge of lava started in May 1991. Then, it has gradually decreased until 1995. The intensity as of 1995 is smaller than that in 1986. This means that magma supply from deeper portion than C-source had already started before 1986, and magma stored at C-source is transported through B-source up to the near-surface A-source, and discharge at the summit.

We may draw one model on the magma supply system at Mt. Unzen as illustrated in Fig. 14. Considering the range of relative intensity changes at each pressure source (A-source: 0.1, B-source: 0.4, and C-source: 6), the size of C-source may be much larger than those of B- and A- sources.

There is still a remained problem. Since the discharge of lava stopped in early 1995, there are no significant change in intensity of B- and C- sources. This suggests that magma supply to C-source which started before 1986 stopped in 1994. Then when does the magma supply stopped? How much magma was supplied from deeper portion to C-source related to the recent activity. These problem are discussed in the next paragraph.

Table. 2 Top: Extrusion lava and magma supply at Mt. Unzen. Volume changes in magma reservoir determined by assuming that the deformation volume are equal to the volume changes in magma reservoir. Bottom: Magma supply rate to the sources A, B and C, respectively.

Period	VOLUME ($10^6 m^3$)						
	Magma discharge	Changes of A source	Magma supply to A source	Change of B source	Magma supply to B source	Change of C source	Magma supply to C source
	Vd	ΔVA	V1	ΔVB	V2	ΔVC	VS
Nov '86 - Nov '90	0					3.73	3.73
Nov '90 - Mar '91	0					10.77	10.77
Mar '91 - Aug '91	25.42	-0.64	24.78	2.75	27.53	-9.88	17.65
Aug '91 - Oct '91	17.15	0.28	17.43	-0.78	16.65	-5.74	10.91
Oct '91 - Dec '91	22.24	0.19	22.43	0.59	23.02	-3.87	19.15
Dec '91 - Feb '92	16.52	-0.03	16.49	-0.53	15.96	-0.17	15.79
Feb '92 - May '92	15.96	-0.22	15.74	-1.80	14.16	-5.08	9.09
May '92 - Sep '92	16.54	-0.02	16.52	-0.11	16.41	1.28	17.70
Sep '92 - Feb '93	15.12	0.19	15.31	0.32	15.64	-0.91	14.72
Feb '93 - Aug '93	26.34	-0.33	26.01	0.52	26.53	-8.94	17.59
Aug '93 - Feb '94	27.66	0.21	27.87	1.64	29.51	-5.79	23.73
Feb '94 - Sep '94	11.5	-0.07	11.43	-2.82	8.61	2.86	11.47
Sep '94 - Feb '95	1.66	-0.02	1.64	0.19	1.83	1.22	3.05
Feb' 95 - Feb' 96	0	-0.04	-0.05	0.19	0.14	-2.54	-2.41
Total	196.11	-0.50	195.60	0.17	195.99	-37.54	158.45

Period	Magma supply rate to ($10^4 m^3$/day)		
	A source	B source	C source
Nov '86 - Nov '90			0.26
Nov '90 - Mar '91			11.97
Mar '91 - Aug '91	29.50	32.77	21.02
Aug '91 - Oct '91	30.58	29.21	19.13
Oct '91 - Dec '91	32.51	33.36	27.76
Dec '91 - Feb '92	27.12	26.20	26.32
Feb '92 - May '92	15.28	13.75	8.82
May '92 - Sep '92	13.54	13.45	14.51
Sep '92 - Feb '93	11.10	11.33	10.67
Feb '93 - Aug '93	15.21	15.52	10.29
Aug '93 - Feb '94	14.44	15.17	12.36
Feb '94 - Sep '94	4.65	3.42	4.66
Sep '94 - Feb '95	1.64	1.77	3.58
Feb' 95 - Feb' 96	-0.01	0.04	-0.67

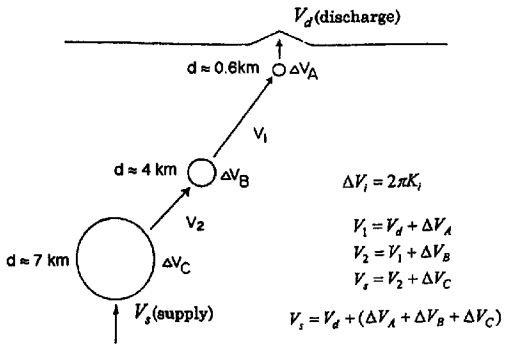

Fig. 14 Schematic diagram for the calculation of magma supply at Mt. Unzen.

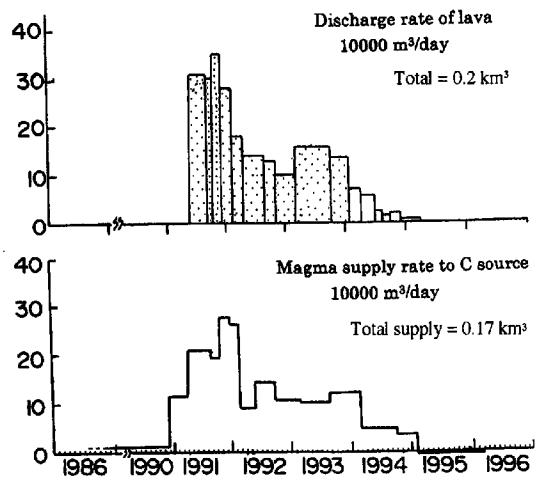

Fig. 15 Discharge rate of lava and the magma supply rate from deeper portion to C source.

5.3 Magma supply from deeper portion to C-source

We now consider the magma supply to C and the transportation through B and A-sources up to the ground surface according to the model as illustrated in Fig. 14. By adding the volume changes in A, B and C-sources and the volume of lava discharged from the summit, we may estimate the magma supply and transportation between the A, B and C-sources, as represented below:

$$\begin{aligned} V_1 &= V_d + \Delta V_A \\ V_2 &= V_1 + \Delta V_B \\ V_S &= V_2 + \Delta V_C \end{aligned} \qquad (9)$$

where, V_d is magma discharge to surface, V_1 is magma supply to A-source, V_2 is magma supply to B-source, and V_s is magma supply to C-source, respectively. ΔV_A, ΔV_B and ΔV_C are the changes in volume of the A, B and C chambers associated with the inflation/deflation of the sources.

Deformation volume of the ground surface may be estimated from the intensity parameters of the leveling model. This was done by integrating over the vertical displacement equation of the point source model, and it equals 2 π K where K is the intensity parameter (Eaton, 1962).

Assuming that volume changes at the surface are equal to changes in magma volume at each source, we estimated V_1, V_2 and Vs for each period of leveling survey. The results of calculation and the estimated rate of magma supply are given in Table 2. The magma supply from deeper portion to C-source increased until the end of 1991, then decayed with time until no supply in 1995, as illustrated in Fig. 15.

The total volume of magma supplied from deeper portion since 1990 is estimated to be about 0.17 km^3. The magma supply rate from May 1991 to February 1995 was about 0.04 km^3/year on average which is, about 2 times larger than that of the results estimated by the previous studies (Ishihara, 1993). However, he estimated the rate using the data in 1991 and 1992 when magma supply rate was high. Therefore, the estimation in this study does not so contradict with his result.

6. Conclusions

From analysis, assuming Point-Source Model to the leveling data at Mt. Unzen, we may conclude that:

[1] Surface ground deformation at Mt. Unzen may be induced by the three pressure sources A, B and C connected with each other.

[2] The supply rate of magma from deeper portion to the deepest source C increased rapidly after the phreatic eruption on November 1990, and reached its peak in the end of 1991, then decayed with time until no magma supply in early 1995. The total volume of magma supplied since 1990 is estimated to be 0.17 km^3. The magma of 0.03 km^3 stored under Mt. Unzen before 1990 was consumed by the eruption.

Acknowledgments

The authors would like to expressed his gratitude thanks to Emeritus Prof. Kosuke Kamo and staff members of Sakurajima Volcano Research Center who gave worthy advise and supports. Their gratitude thanks are expressed to Joint Research Team of Mt. Unzen and Geographical Survey Institute for their

expertise in performing a careful and timely job leveling at Mt. Unzen.

Their sincere thanks to: The Director of Volcanological Survey of Indonesia (VSI) Dr. Wimpy S. Tjetjep who give worthy advise and support. Thanks also to Dr. R. Sukhyar, Dr. Surono and all staff of VSI for their supports.

References

Bomford, G. (1971) Geodesy. Oxford Univ. Press, New York, NY, 731p.

Eaton, JP. (1962) Crustal structure and volcanism in Hawaii. *Am. Geophys Union Geophys. Monogr.*, Vol. 6, pp. 13-29.

Ishihara, K. (1993) Continuous magma supply inferred from discharge rate of magma and ground deformation rate at Mt. Unzen, Japan. *Annuals. Disas. Prev. Res. Inst. Kyoto Univ.*, Vol. 36B-1, pp. 219－230 (in Japanese with English abstract).

Geodetic Survey Group (1994) Pressure source under Unzen Volcano inferred from vertical displacement, Program and Abstracts, *Volcanol. Soc. Japan*, 1994, No. 2.

Geographical Survey Institute (1994) Data for the 67th meeting of Coordinating Committee for Prediction of Volcanic Eruption, pp. 6-7.

Goelogical Survey of Japan; Unzendake Weather Station, JMA; and Onokiba Primary School, Hukae Town (1995) Ground deformation of Fugen-dake, Unzen Volcano, measured by EDM between January 1995 and May 1995. *Rept. Coordinating Committee for Prediction of Volcanic Eruption*, No. 62, pp. 35-37

Mogi, K. (1958) Relation between the eruption of various volcanoes and the deformations of the ground surface around them. *Bull. Earthq. Res. Inst., Tokyo Univ.*, Vol. 36, pp. 99-134.

Nishi, K. Ono, H. Mori, H. Matsushima, T. and Ohmi, S. (1995) GPS measurements of ground deformation associated with magma intrusion and lava discharge at Unzen Volcano. *Proceedings of the Japanese Symposium on GPS*, pp. 99-105.

Ohta, K. (1993) A study of hot springs on the Shimabara Peninsula. Sci., Rept. Shimabara Volcano Observatory., *Fac. Sci., Kyushu Univ.*, Vol. 8, pp. 1-33 (in Japanese with English abstract).

Ohta, K. Matsuo, N and Yanagi, T. (1992) The 1990-1992 eruption of Unzen Volcano. in *Unzen Volcano, The 1990-1992 Eruption*, The Nishi nippon & Kyushu Univ. Press, pp.38-43

Shimizu, H. Umakoshi, K. Matsuo, N. and Ohta, K. (1992) Seismological observation of Unzen Volcano before and during the 1990-1992 eruption. in *Unzen Volcano, The 1990-1992 Eruption*, The Nishi nippon & Kyushu Univ. Press, pp.34-37.

Umakoshi, Shimizu, H. and Matsuo, N. (1995) Magma storages at Mt. Unzen, as inferred from precisely determined hypocentral distribution. Preliminary Research on Prospecting the subsurface structure of Mt. Unzen (ed. Ohta, K.), pp. 47-52.

要旨

1990年11月に198年ぶりに噴火活動を開始した雲仙普賢岳は、1991年5月20日からデイサイト質溶岩を噴出し、1995年始めまで、溶岩噴出と火砕流発生を繰り返した。国立大学総合研究班および国土地理院は、雲仙普賢岳の北山麓から山頂へ向かう路線、および島原半島西岸沿いの路線に沿って水準測量を繰り返してきた。また、GPS 観測も繰り返された。その結果、島原半島西部の地盤は溶岩流出まで隆起・膨張し、溶岩流出開始後沈降・収縮に転じたことがわかった。これまでの研究によって、普賢岳山頂の直下から西に向かって次第に深さを増す、3つの圧力源、A、BおよびCを仮定すれば雲仙岳周辺の地盤の変動が説明できることが示された。

本研究では、水準測量データの測定誤差を考慮した上で、点力源モデルを適用して、3つの圧力源の位置、およびそれぞれの圧力源の強度の時間的変化を再計算した。その上で、溶岩噴出率および地震活動と圧力源の強度の関係、また、地盤の変形体積と溶岩噴出率をもとに地下深部からのマグマ供給率を推定した。

[1] 普賢岳火口の地下 1.4km に力源 A、普賢岳の西方約 3km、深さ 4.1km に力源 B、および普賢岳西方約 5km、深さ 6.8km に力源 C の存在が推定された。各力源は島原半島西方の橘湾から普賢岳に伸びる地震帯の直下に位置する。

[2] 溶岩噴出開始以降、普賢岳直下の力源 A の強度の変化は、溶岩噴出率と普賢岳の地震活動の増減と対応している。

[3] 力源 B の強度の変化は溶岩噴出率の 2 度の増大に対応している。一方、力源 C の強度は溶岩流出開始まで増大し、その後は時間とともに減少している。

[4] 以上の結果より、マグマが力源 C から、力源 B および力源 A を経由して輸送され、普賢岳山頂から噴出したことが推定される。地盤の変動体積の変化が力源でのマグマ蓄積量の増減に等しいと仮定して、地下深部から力源 C へのマグマ供給率を推定した。マグマ供給率は、溶岩噴出開始の約半年前から急増し、1991 年終わりにピークに達し、それ以後減少して、1995 年始めには停止した。1990 年から 1995 年までのマグマ供給量は 0.17km^3 と推定される。

キーワード:雲仙火山、水準測量、圧力源、マグマ供給率、溶岩ドーム